

Compact Representation of Uncertainty in Hierarchical Clustering

Craig S. Greenberg^{*,1,2}, Sebastian Macaluso^{*,3}, Nicholas Monath¹, Ji-Ah Lee⁴,
 Patrick Flaherty⁴, Kyle Cranmer³, Andrew McGregor¹, and Andrew McCallum¹

¹College of Information and Computer Sciences, University of Massachusetts Amherst, USA

²National Institute of Standards and Technology, USA

³Center for Cosmology and Particle Physics & Center for Data Science, New York University, USA

⁴Department of Mathematics and Statistics, University of Massachusetts Amherst, USA

Keywords: Hierarchical Clustering – Jet Physics – Genomics

Abstract

Hierarchical clustering is a fundamental task often used to discover meaningful structures in data, such as phylogenetic trees, taxonomies of concepts, subtypes of cancer, and cascades of particle decays in particle physics. When multiple hierarchical clusterings of the data are possible, it is useful to represent uncertainty in the clustering through various probabilistic quantities, such as the distribution over tree structures and the marginal probabilities of subtrees. Existing approaches represent uncertainty for a range of models; however, they only provide *approximate* inference. This paper presents dynamic-programming algorithms and proofs for *exact* inference in hierarchical clustering at small but useful scales. We are able to compute the partition function, MAP hierarchical clustering, and marginal probabilities of sub-hierarchies and clusters. Our method supports a wide range of hierarchical clustering models and only requires a cluster compatibility function. Rather than scaling with the number of hierarchical clusterings of N elements $((2N - 3)!!)$, our approach runs in time and space proportional to the significantly smaller powerset of N . Despite still being large, there are many important applications at the practically-computable range of $N < 20$. We demonstrate the advantages of exact inference on synthetic data of interest to Dasgupta’s cost [16] as well as on two real world applications, in particle physics at the Large Hadron Collider at CERN and in cancer genomics.

^{*}Both authors contributed equally to this work.

Corresponding authors: Craig S. Greenberg , Sebastian Macaluso
 csgreenberg@cs.umass.edu, sm4511@nyu.edu

1 Introduction

Hierarchical clustering is often used to discover meaningful structures, such as phylogenetic trees of organisms [24], taxonomies of concepts [9], subtypes of cancer [33], and jets in particle physics [5]. Among the reasons that hierarchical clustering has been found to be broadly useful is that it forms a natural data representation of data generated by a Markov tree, i.e., a tree-shaped model where the state variables are dependent only on their parent or children. Additionally, hierarchical clusterings can be used to represent alternative flat partitions of a dataset.

Often, probabilistic approaches, such as diffusion trees [27, 22] and coalescent models [36, 4, 20], model which tree structures are likely for a given dataset. For instance, in particle physics generative models of trees are used to model jets [5], and similarly coalescent models have been used in phylogenetics [34]. Inference in these approaches is done by approximate, rather than exact, methods such as greedy best-first, beam-search, sequential Monte Carlo [39], and MCMC [27] and lead to local optima. These methods do not have efficient ways to compute an exact normalized distribution over all tree structures.

Despite this, modeling distributions over tree structures has been the subject of a large body of work, including various types of Bayesian non-parametric models, e.g., [22, 20, 2, 28, 17]. These methods only support using parametric distributions to define emission probabilities and do not support the general family of potential functions as in our method. Bootstrapping methods, such as [35], represent uncertainty in hierarchical clustering, however they approximate statistics of interest through repeatedly (re-)sampling from the empirical distribution. Recent work [21, 23, 19] has studied distributions over flat clusterings and showed that dynamic programming can be used to both efficiently compute the partition function as well as find the MAP clustering [38, 18]. However, analogous results for hierarchical clustering were not known.

In this paper, we provide data structures and algorithms for efficiently computing exact distributions over hierarchical clusterings. We show how these methods can be used to produce not only a normalizing constant for the distribution but also find the MAP clustering, as well as compute marginal distributions, including the probability of any sub-hierarchy or cluster. We further show how to sample exactly from the posterior distribution over hierarchical clusterings (i.e., the probability of sampling a given hierarchy is equal to the probability of that hierarchy). Our methods require time and space subquadratic in the powerset of N , a substantial reduction over brute force methods, which require $(2N - 3)!!$, making practical exact inference for datasets on the order of 20 points ($\sim 10^{22}$ trees) or fewer, thereby benefiting real-world use cases where exact inference on datasets this size is of high interest and practical importance. For example, in jet physics there are practical applications for datasets of this size when implementing simplified models for the cascades of particle decays [31, 32] or on experimental data (after preprocessing methods) from proton-proton collisions at the Large Hadron Collider at CERN. We demonstrate our methods' capabilities for exact inference in discovering cascades of particle decays in jet physics and subtype

hierarchies in cancer genomics, two applications where there is a need for exact inference on datasets made feasible by our methods. We find that greedy and beam search methods frequently return estimates that are sub-optimal compared to the exact MAP clustering, and we quantify exactly various probabilistic quantities of interest in these domains, only made possible by our methods.

2 Probabilistic Models for Hierarchical Clustering

A hierarchical clustering is a recursive splitting of a dataset into subsets until reaching singletons (this can equivalently be viewed as starting with the set of singletons and repeatedly taking the union of sets until reaching the entire dataset). This is in contrast to flat clustering, where the task is to partition the dataset into disjoint subsets. Formally,

Definition 1. (Hierarchical Clustering¹) *Given a dataset of elements, $X = \{x_i\}_{i=1}^N$, a **hierarchical clustering**, \mathbb{H} , is a set of nested subsets of X , s.t. $X \in \mathbb{H}$, $\{\{x_i\}\}_{i=1}^N \subset \mathbb{H}$, and $\forall X_i, X_j \in \mathbb{H}$, either $X_i \subset X_j$, $X_j \subset X_i$, or $X_i \cap X_j = \emptyset$. Further, $\forall X_i \in \mathbb{H}$, if $\exists X_j \in \mathbb{H}$ s.t. $X_j \subset X_i$, then $\exists X_k \in \mathbb{H}$ s.t. $X_j \cup X_k = X_i$.*

When a subset $X_j \in \mathbb{H}$, X_j is referred to as a cluster in \mathbb{H} . When $X_i, X_j, X_k \in \mathbb{H}$ and $X_j \cup X_k = X_i$, we refer to X_j and X_k as children of X_i , and X_i the parent of X_j and X_k ; if $X_j \subset X_i$ we refer to X_i as an ancestor of X_j and X_j a descendent of X_i . Leaves of the tree refer to individual elements / singleton clusters.

In our work, we consider an energy-based probabilistic model for hierarchical clustering. We provide a general (and flexible) definition of the probabilistic model and then give three specific examples of the distribution. Our model is based on measuring the compatibility of all pairs of sibling nodes in a binary tree structure. Formally,

Definition 2. (Energy-based Hierarchical Clustering) *Let X be a dataset, \mathbb{H} be a hierarchical clustering of X , let $\psi : 2^X \times 2^X \rightarrow \mathbb{R}^+$ be a potential function describing the compatibility of a pair of sibling nodes in \mathbb{H} , and let $\phi(\mathbb{H})$ be a potential function for the \mathbb{H} structure. Then, the probability of \mathbb{H} for the dataset X , $P(\mathbb{H}|X)$, is equal to the unnormalized potential of \mathbb{H} normalized by the partition function, $Z(X)$:*

$$P(\mathbb{H}|X) = \frac{\phi(\mathbb{H})}{Z(X)} \text{ where } \phi(\mathbb{H}) = \prod_{X_L, X_R \in \text{sibs}(\mathbb{H})} \psi(X_L, X_R) \quad (1)$$

where $\text{sibs}(\mathbb{H}) = \{(X_L, X_R) | X_L \in \mathbb{H}, X_R \in \mathbb{H}, X_L \cap X_R = \emptyset, X_L \cup X_R \in \mathbb{H}\}$ and the partition function $Z(X)$ is given by:

$$Z(X) = \sum_{\mathbb{H} \in \mathcal{H}(X)} \phi(\mathbb{H}). \quad (2)$$

¹We limit our exposition to binary hierarchical clustering. Binary structures encode more tree-consistent clusterings than k-ary [3]. Natural extensions may exist for k-ary clustering, which are left for future work.

where $\mathcal{H}(X)$ gives all binary hierarchical clusterings of the elements X . We refer to this as an energy-based model since often it is the case that $\psi(\cdot, \cdot)$ is defined by the unnormalized Gibbs distribution, as $\psi(X_L, X_R) = \exp(-\beta E(X_L, X_R))$, where β is the inverse temperature and $E(\cdot, \cdot)$ is the energy.

This probabilistic model allows us to express many familiar distributions over tree structures. It also has a connection to the classic algorithmic hierarchical clustering technique, agglomerative clustering, in that $\psi(\cdot, \cdot)$ has the same signature as a “linkage function” (i.e., single, average, complete linkage). We note that in this work we do not use informative prior distributions over trees $P(\mathbb{H})$ and instead assume a uniform prior. We now give three example instances of the aforementioned probabilistic model:

Example 1. (Jet Physics) The potential of a hierarchy is identified with the product of the likelihoods of all the $1 \rightarrow 2$ splittings of a parent cluster into two child clusters in the binary tree. Each cluster, X , corresponds to a particle with an energy-momentum vector $x = (E \in \mathbb{R}^+, \vec{p} \in \mathbb{R}^3)$ and squared mass $t(x) = E^2 - |\vec{p}|^2$. A parent’s energy-momentum vector is obtained from adding its children, i.e., $x_P = x_L + x_R$. We study a toy model for jet physics, where for each pair of parent and left (right) child clusters, with masses $\sqrt{t_P}$ and $\sqrt{t_L}$ ($\sqrt{t_R}$) respectively, the likelihood function is,

$$\psi(X_L, X_R) = f(t(x_L)|t_P, \lambda) \cdot f(t(x_R)|t_P, \lambda) \quad (3)$$

where

$$f(t|t_P, \lambda) = \frac{1}{1 - e^{-\lambda}} \frac{\lambda}{t_P} e^{-\lambda \frac{t}{t_P}} \quad (4)$$

The first term is a normalization factor associated to the constraint that $t < t_P$.

Example 2. (Hierarchical Correlation Clustering) In the cancer genomics use case (§4.2), we are given a dataset of vectors indicating level of gene expressions which are endowed with pairwise affinities that are both positive and negative. In this case, we define the energy of a pair of sibling nodes in the tree to be the sum of the positive edges not crossing the cut, minus the sum of the negative edges crossing the cut. Let w_{ij} be the affinity between x_i and x_j :

$$\psi(X_i, X_j) = \exp(-\beta E(X_i, X_j)) \quad (5)$$

$$E(X_i, X_j) = \sum_{\substack{x_i, x_j \in X_i \times X_j}} w_{ij} \mathbb{I}[w_{ij} > 0] - \sum_{\substack{x_i, x_j \in X_i \times X_i, \\ x_i \neq x_j}} w_{ij} \mathbb{I}[w_{ij} < 0] - \sum_{\substack{x_i, x_j \in X_j \times X_j, \\ x_i \neq x_j}} w_{ij} \mathbb{I}[w_{ij} < 0] \quad (6)$$

This energy is the correlation clustering objective [1].

Example 3. (Dasgupta’s Cost) Dasgupta [16] defines a cost function for hierarchical clustering that has been the subject of much theoretical interest (primarily on approximation algorithms for the cost) [10, 11, 7, 8, 26, 30]. Given a graph with vertices of the dataset X

and weighted edges representing pairwise similarities between points $\mathcal{W} = \{(i, j, w_{ij}) | i, j \in \{1, \dots, |X|\} \times \{1, \dots, |X|\}, i < j, w_{ij} \in \mathbb{R}^+\}$. Dasgupta's cost is defined as:

$$E(X_i, X_j) = (|X_i| + |X_j|) \sum_{x_i, x_j \in X_i \times X_j} w_{ij} \quad (7)$$

This is equivalent to the cut-cost definition of Dasgupta's cost with the restriction to binary trees [16].

2.1 Contributions of this Paper

For the given probabilistic model for hierarchical clustering, we would like to achieve *exact*, not approximate, solutions to the following:

Compute the Partition Function $Z(X)$ and thereby the distribution of hierarchical clusterings.

MAP Inference Find the tree structure: $\text{argmax}_{\mathbb{H} \in \mathcal{H}} P(\mathbb{H}|X)$.

Sample Hierarchies from the Posterior Distribution i.e., weighted by their probability, $P(\mathbb{H}|X)$.

3 Cluster Trellis for Hierarchical Clustering

Exactly performing MAP inference and finding the partition function by enumerating all hierarchical clusterings over N elements is exceptionally difficult because the number of hierarchies grows extremely rapidly, namely $(2N - 3)!!$ (see [6, 15] for more details and proof), where $!!$ is double factorial. To overcome the computational burden, we introduce a cluster trellis data structure [18] for hierarchical clustering. We describe how this data structure enables us to use dynamic programming algorithms to exactly compute MAP structures and the partition function. Our algorithms compute these quantities without having to iterate over each possible hierarchy in the $\mathcal{O}(3^N)$ time. While still exponential, this is orders of magnitude faster than enumerating all trees and is to our knowledge the fastest exact MAP / partition function result (See §A.5 and §A.7 for proofs). Furthermore, we demonstrate how our methods can be used to sample structures from $P(\mathbb{H}|X)$, compute marginal probabilities of subtrees, all without enumerating the complete set of hierarchical clusterings.

3.1 Trellis Data Structure

The trellis data structure is a directed acyclic graph, where there is a bijection between the vertices of the graph and $\mathbb{P}(X)$, and there is an edge from vertex \mathbb{V}_i to vertex \mathbb{V}_j when the set of elements associated with \mathbb{V}_j is a maximal superset of the set of elements associated

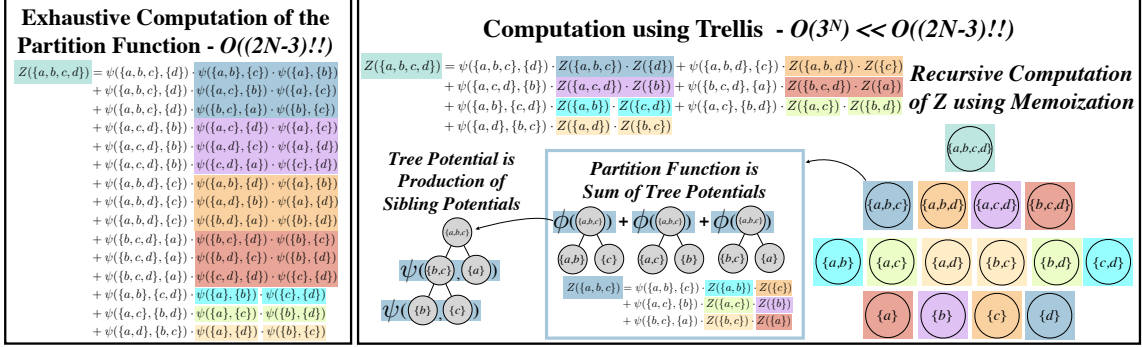


Figure 1: **Computing the partition function.** An example of using a trellis to compute the distribution over hierarchical clusterings of the dataset $\{a, b, c, d\}$. The left panel shows the exhaustive computation of the partition function, consisting of the summation of $(2 \cdot 4 - 3)!! = 15$ trees rooted at $\{a, b, c, d\}$. The right panel shows the computation of the partition function using the corresponding trellis. The sum for the partition function is over $2^{4-1} - 1 = 7$ equations, each making use of a memoized Z value. Colors indicate corresponding computations that are computed with and stored in the trellis.

with \mathbb{V}_i . The dataset associated with a trellis vertex \mathbb{V} is denoted $X(\mathbb{V})$ and the trellis vertex associated with a dataset X is denoted $\mathbb{V}(X)$. Each node in the trellis will store memoized values of $Z(\mathbb{V})$ for computing the partition function and the value $\phi(H^*[\mathbb{V}])$ and the backpointer $\Xi(H^*[\mathbb{V}])$ for computing the MAP tree. We note that the edges of the structure are not crucial for presentation here. However they are practically useful in the implementation of the trellis and provide a parallel between the trellis structure and a DAG structure and the tree structure given by a hierarchical clustering.

3.2 Computing the Partition Function

Given a dataset of elements, $X = \{x_i\}_{i=1}^N$, the partition function, $Z(X)$, for the set of hierarchical clusterings over X , $\mathcal{H}(X)$, is given by Equation 2. The trellis is used to facilitate a memoized dynamic program to compute the partition function and the MAP. To achieve this, we need to re-write the partition function in the corresponding recursive way. In particular,

Proposition 1. *For any $x \in X$, the hierarchical partition function can be written recursively, as $Z(X) = \sum_{H \in \mathcal{H}(X)} \phi(H) = \sum_{X_i \in X_x} \psi(X_i, X \setminus X_i) \cdot Z(X_i) \cdot Z(X \setminus X_i)$ where X_x is the set of all clusters containing the element x (omitting X), i.e., $X_x = \{X_j : X_j \in 2^X \setminus X \wedge x \in X_j\}$.*

The proof is given in § A.1 in the Appendix. Algorithm 1 describes how to efficiently compute the partition function using the trellis by making use of Proposition 1. Our

Algorithm 1 PartitionFunction(X)

```
Pick  $x_i \in X$  and set  $Z(X) \leftarrow 0$ 
for  $X_j$  in  $2^{X \setminus \{x_i\}}$  do
     $X_i \leftarrow X_j \cup \{x_i\}$ 
    if  $Z(\mathbb{V}(X_i))$  not set then  $Z(\mathbb{V}(X_i)) \leftarrow \text{PartitionFunction}(X_i)$ 
    if  $Z(\mathbb{V}(X \setminus X_i))$  not set then  $Z(\mathbb{V}(X \setminus X_i)) \leftarrow \text{PartitionFunction}(X \setminus X_i)$ 
     $Z(X) \leftarrow Z(X) + \psi(X_i, X \setminus X_i) \cdot Z(\mathbb{V}(X_i)) \cdot Z(\mathbb{V}(X \setminus X_i))$ 
return  $Z(X)$ 
```

algorithm works by first setting the partition function of the leaf nodes in the trellis to 1. Algorithm 1 is described in a recursive way. It starts by picking any element in the dataset, x_i , and the complement containing all points other than x_i , $X \setminus x_i$. It then considers all clusters, X_j , of the powerset of $X \setminus x_i$, i.e., $X_j \in 2^{X_j \setminus x_i}$. For the cluster $X_i = X_j \cup \{x_i\}$, the partition function is computed (memoized, recursively) for X_i and its complement, thus enabling the application of Proposition 1 to get $Z(X)$. The algorithm can equivalently be written in a bottom-up, non-recursive way. In this case, the partition function for every node in the trellis is computed in order (in a bottom-up approach), from the nodes with the smallest number of elements to the nodes with the largest number of elements, memoizing the partition function value at each node. By computing the partition functions in this order, whenever computing the partition function of a given node in the trellis, the partition functions of all of the descendent nodes will have already been computed and memoized. In Figure 1, we show a visualization comparing the computation of the partition function with the trellis to the brute force method for a dataset of four elements. We have the following complexity result for the algorithm:

Theorem 1. *For a given dataset X of N elements, Algorithm 1 computes $Z(X)$ in $\mathcal{O}(3^N)$ time.*

The proof is given in § A.7 in the Appendix. The time-complexity of the algorithm is $\mathcal{O}(3^N)$, since the partition function for each node in the trellis is computed and the descendent nodes' partition functions are always pre-computed due to the order of computation. This is significantly smaller than the $(2N - 3)!!$ possible hierarchies.

3.3 Computing the MAP Hierarchical Clustering

Similar to other dynamic programming algorithms, such as Viterbi, we can adapt Algorithm 1 in order to find the MAP hierarchical clustering. The MAP clustering for dataset X , $\mathbb{H}^*(X)$, is $\mathbb{H}^*(X) = \text{argmax}_{\mathbb{H} \in \mathcal{H}(X)} P(\mathbb{H}|X) = \text{argmax}_{\mathbb{H} \in \mathcal{H}(X)} \phi(\mathbb{H})$. As in the partition function, we can use a recursive memoized technique. Each node will store a value for the MAP, denoted $\phi(\mathbb{H}^*(X))$ and a backpointer $\Xi(\mathbb{H}^*(X))$. To use the recursive technique we use the following Proposition for correctness of the recursion.

Proposition 2. For any $x \in X$, let $X_x = \{X_j : X_j \in 2^X \setminus X \wedge x \in X_j\}$, then $\phi(\mathbb{H}^*(X)) = \max_{X_i \in X_x} \psi(X_i, X \setminus X_i) \cdot \phi(\mathbb{H}^*(X_i)) \cdot \phi(\mathbb{H}^*(X \setminus X_i))$.

See §A.6 in the Appendix for proof. As in the partition function algorithm described in Section 3.2, the time complexity for finding the MAP clustering is $\mathcal{O}(3^N)$. To compute the maximal likelihood hierarchical clustering, the maximal energy of the sub-hierarchy rooted at each node is computed, rather than the partition function. Pointers to the children of the maximal sub-hierarchy rooted at each node are stored at that node. A proof of the time complexity, analogous to the one for the partition function, can be found in §A.5 of the Appendix.

3.4 Marginals

In this section, we describe how to compute two types of marginal probabilities. The first is for a given sub-hierarchy rooted at X_i , i.e., $\mathbb{H}_i \in \mathcal{H}(X_i)$, defined as $P(\mathbb{H}_i|X) = \sum_{\mathbb{H} \in A(\mathbb{H}_i)} P(\mathbb{H}|X)$, where $A(\mathbb{H}_i) = \{\mathbb{H} : \mathbb{H} \in \mathcal{H}(X) \wedge \mathbb{H}_i \subset \mathbb{H}\}$, and $\mathbb{H}_i \subset \mathbb{H}$ indicates that \mathbb{H}_i is a subtree of \mathbb{H} . The second is for a given cluster, X_i , defined as $P(X_i|X) = \sum_{\mathbb{H}_i \in \mathcal{H}(X_i)} P(\mathbb{H}_i|X)$. The value of $P(\mathbb{H}_i|X_i)$ can be computed using the same algorithm used for the partition function, except by first merging $X(\mathbb{H}_i|X)$ into a single leaf node, but using $\phi(X(\mathbb{H}_i))$ for the energy of the newly merged leaf. The same is true for computing the value of $P(X_i|X)$, except after merging X_i into a single leaf node, the value $Z(X_i)$ should be used. See Appendix § A.4 for proofs.

3.5 Sampling from the Distribution over Trees

Drawing samples from the true posterior distribution $P(\mathbb{H}|X)$ is also difficult because of the extremely large number of trees. In this section, we introduce a sampling procedure for hierarchical clusterings \mathbb{H}_i implemented using the trellis which gives samples from the true posterior without enumerating all possible hierarchical clusterings.

The sampling procedure will build a tree structure in a top-down way. We start with the cluster of all the elements, X , and then sample one child of that cluster, $X_L \subset X$, (Eq. 8) and set the other to be the complement of the child with respect to the parent, i.e., $X \setminus X_L$. This procedure repeats recursively from each of the children and terminates when a cluster contains a single element. A child X_L of parent X_p , i.e., $X_L \subset X_p$ is sampled according to:

$$p(X_L|X_p) = \frac{1}{Z(X_p)} \cdot \psi(X_L, X_p \setminus X_L) \cdot Z(X_L) \cdot Z(X_p \setminus X_L). \quad (8)$$

Pseudocode for this algorithm is given in Algorithm 2.

Theorem 2. `Sample`(X) (Alg. 2) gives samples from $P(\mathbb{H}|X)$.

The proof is given in Appendix § A.2. This algorithm is notable in that it does not require computing a categorical distribution over all trees and samples exactly according to $P(\mathbb{H}|X)$.

Algorithm 2 `Sample(X)`

```
if  $|X| = 1$  return  $\{X\}$ 
Sample  $X_L$  from  $p(X_i|X)$  (Eq. 8).
return  $\{X_L, X \setminus X_L\} \cup \text{Sample}(X_L) \cup \text{Sample}(X \setminus X_L)$ 
```

4 Experiments

In this section, we demonstrate the use of the exact MAP, partition function, and sampling approaches described in this paper on two real world applications: jet physics and cancer genomics, as well as one synthetic data experiment related to Dasgupta’s cost [16]. In each real world application, we demonstrate how the trellis is used to compute exact MAP and the distribution over clusterings that are more informative and accurate than approximate methods. In particle physics, we use a simulation model for cascades of particle physics decays in jet physics that provides ground truth hierarchies facilitating evaluation. We additionally demonstrate the use of the sampling procedure (§3.5) in this domain. In cancer genomics, we show how we can model subtypes of cancer, which can help determine prognosis and treatment plans. Lastly, we give an illustrative example for the use of the proposed approaches with Dasgupta’s cost, running on the kinds of data for which greedy methods are known to be approximate.

4.1 Jet Physics and Hierarchical Clusterings

Background The Large Hadron Collider (LHC) at CERN collides two beams of high-energy protons and produces many new (unstable) particles. Some of these new particles (quarks and gluons) will undergo a *showering process*, where they radiate many other quarks and gluons in successive binary splittings. These $1 \rightarrow 2$ splittings can be represented with a binary tree, where the energy of the particles decreases after each step. When the energy is below a given threshold, the showering terminates, resulting in a spray of particles that is called a *jet*. The particle detectors only observe the leaves of this binary tree (the jet constituents), and the unstable particles in the showering process are unobserved. Thus, a specific jet could result from several latent trees generated by the showering process. While the latent showering process is unobserved, it is described by quantum chromodynamics (QCD).

Data and Methods In this paper, we proposed a new method to efficiently find the MAP hierarchical clustering, partition function Z , and compute an estimate for the posterior distribution over all possible hierarchical clusterings from sampling. We will compare the trellis results for the MAP hierarchical clustering with approximate methods, as described below. The ground truth hierarchical clusterings of our dataset are generated with the toy generative model for jets Ginkgo, see [12] for more details. This model implements a

| | BEAM SEARCH | GREEDY |
|-------------|---------------|---------------|
| TRELLIS | 0.4 ± 0.5 | 1.5 ± 1.1 |
| BEAM SEARCH | | 1.1 ± 1.1 |

Table 1: Mean and standard deviation for the difference in log likelihood for the MAP tree found by algorithms indicated by the row and column heading on the Ginkgo510 dataset.

recursive algorithm to generate a binary tree, whose leaves are the jet constituents. Jet constituents (leaves) and intermediate state particles (inner nodes) in Ginkgo are represented by a four dimensional energy-momentum vector.

Next, we review new algorithms to cluster jets based on the joint likelihood of the jet binary tree in Ginkgo, introduced in [14]. In this work the authors explore algorithms that aim to obtain the maximum likelihood estimate (MLE) or MAP for the latent structure of a jet. In this approach, the tree latent structure z_{shower} is fixed by the algorithm. In particular, greedy and beam search algorithms are studied. Greedy simply chooses the pairing of nodes that locally maximizes the likelihood at each step, whereas beam search maximizes the likelihood of multiple steps before choosing the latent path. The current implementation only takes into account one more step ahead, with a beam size given by $\frac{N(N-1)}{2}$, with N the number of jet constituents to cluster. Also, when two or more clusterings had an identical likelihood value, only one of them was kept in the beam, to avoid counting multiple times the different orderings of the same clustering (see [4] for details about the different orderings of the internal nodes of the tree). This approach significantly improved the performance of the beam search algorithm in terms of finding the MLE.

Results In this section we show results for the implementation of the trellis algorithm on a jet physics dataset of 5000 Ginkgo [13] jets with a number of leaves between 5 and 10, and we refer to it as Ginkgo510. We start by comparing in Table 1 the mean difference among the MAP values for the hierarchies likelihood obtained with the trellis, beam search and greedy algorithms. We see that the likelihood of the trees increase from greedy to beam search to the trellis one, as expected.

We use beam search as a baseline to estimate the MAP value, which typically has a good performance for trees with up to about 10 leaves, but as we see in Table 1, the trellis MAP value is greater. Next, in Figure 2 we show a plot of the partition function versus the MAP for each set of leaves in Ginkgo510 dataset. It is interesting to note that there seems to be a correlation between Z and the Trellis MAP. We want to emphasize that the implementation of the trellis algorithm allows us to access the partition function.

Finally, we show the implementation of the sampling procedure introduced in section 3.5. We compare the sampled posterior distribution with respect to the expected one (as explained below), conditioned on a set of five leaves. We show in Figure 3 the results from sampling 10^5 hierarchies (black dots) and the expected distribution (green) for the likelihood of each hierarchy. The expected posterior is defined as the probability density function of each possible hierarchy. In principle, this could be obtained by taking the ratio of the likelihood of each hierarchy with respect to the partition function Z . We opt to take an

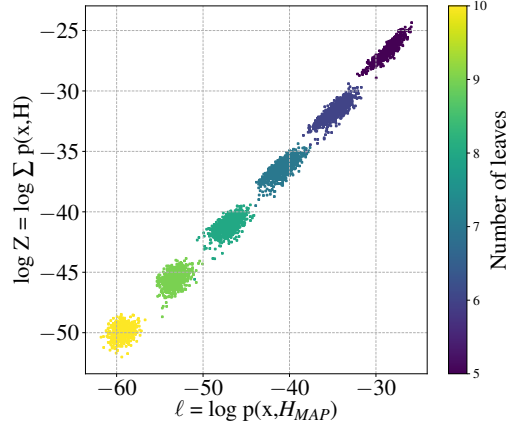


Figure 2: Scatter plot of the partition function Z vs. the trellis MAP ℓ for the Ginkgo510 dataset, with up to 10 leaves (jet constituents). The color indicates the number of leaves of each hierarchical clustering. There appears to be a correlation between Z and the MAP.

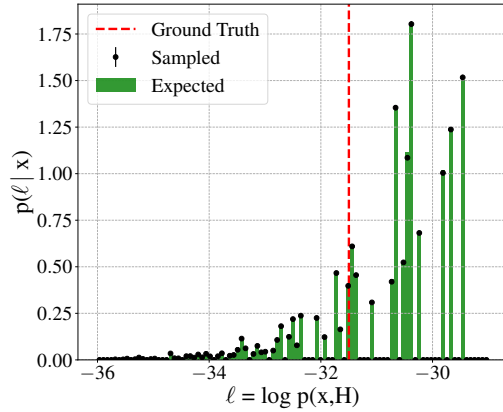


Figure 3: Comparison of the posterior distribution for a specific jet with five leaves for sampling 10^5 hierarchies using Alg 2 (black dots with small error bars) and expected posterior distribution (in green). The plots show the discrete nature of the distribution. The log likelihood for the ground truth tree is a vertical dashed red line.

approximate approach, as follows. If we sample enough number of times, we would expect each possible hierarchy to appear at least once. Thus, as a proof of concept, we sample 10^5 hierarchies for a set of five leaves (88 different hierarchies), keep only one of them for each unique likelihood value and normalize by Z and bin size. We show this result in the histogram labeled as Expected (green) in Figure 3. There is an excellent agreement between the sampled and the expected distributions.

4.2 Cancer Genomics and Hierarchical Clusterings

Background Hierarchical clustering is a common clustering approach for gene expression data [33]. However, standard hierarchical clustering uses a greedy agglomerative or divisive heuristic to build a tree. It is not uncommon to have a need for clustering a small number of samples in cancer genomics studies. An analysis of data available from <https://clinicaltrials.gov> shows that the median sample size for 7,412 completed phase I clinical trials involving cancer is only 30.

Data and Methods Here, we compare a greedy agglomerative clustering to our exact MAP clustering tree using the Prediction Analysis of Microarray 50 (**pam50**) gene expression data set. The **pam50** data set ($n = 232$, $d = 50$) is available from the UNC MicroArray Database [37]. It has intrinsic subtype annotations for 139 of the 232 samples. Missing data

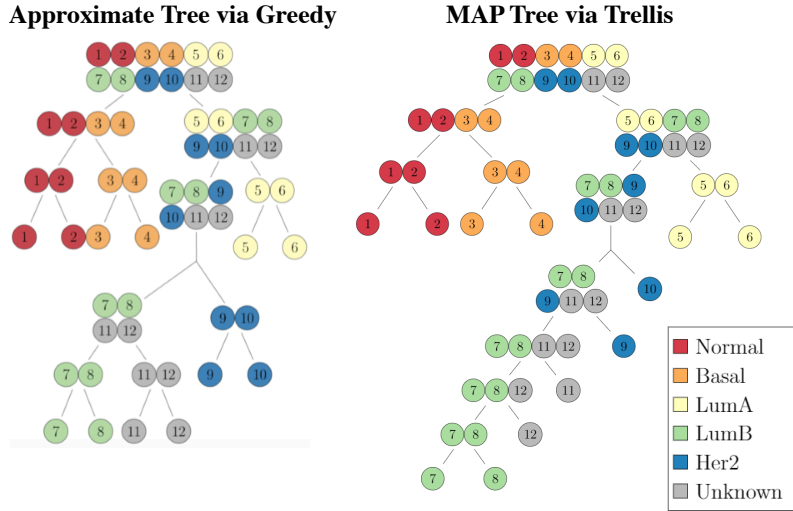


Figure 4: **Cancer Genomics.** Comparison of trees from greedy hierarchical clustering (left) and exact MAP clustering using the trellis (right) on the subsampled `pam50` data set. The colors indicate subtypes of breast cancer (grey if unknown). Though both appear to assign unknown samples to LumB, the right tree positions the unknown samples closer to the Her2 samples.

values (2.65%) were filled in with zeros. We drew a stratified sample of the total data set with two samples from each known intrinsic subtype and two samples from the unknown group. See Appendix § A.8 for more details.

Results Figure 4 displays the greedy hierarchical clustering tree and the MAP tree with transformed weights (see Appendix § A.8 for more details) for the twelve samples selected from the `pam50` dataset. The main difference between these trees is in the split of the subtree including LumB, HER2, and unknown samples. The greedy method splits HER2 from LumB and unknown, while the MAP tree shows a different topology for this subtree. For the MAP solution, we note that the subtree rooted at $\{7, 8, 9, 10, 11, 12\}$ is consistent. All of the correlation coefficients among this cluster are positive, so the optimal action is to split off the item with the smallest (positive) correlation coefficient.

4.3 Dasgupta’s Cost

Figure 5 gives an example graph, as proposed by [8] to bound average-linkage performance, following a model for which greedy methods are known to be approximate with respect to Dasgupta’s cost [26, 10]. We run greedy agglomerative clustering and trellis-based MAP procedure (Eq. 7). Unsurprisingly, the greedy method fails to achieve the lowest cost tree

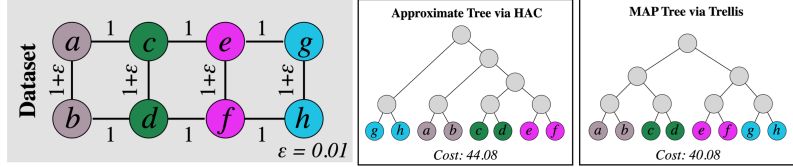


Figure 5: **Dasgupta’s Cost.** Comparison between MAP tree found using the trellis and the tree found by agglomerative clustering for a graph that is known to be difficult for with greedy methods.

while the trellis-based method identifies an optimal tree. The cost of the greedily built tree is 44.08 while the tree built using the trellis is 40.08.

5 Related Work

Modeling distributions over tree structures has been the subject of a large body of work. Bayesian non-parametric models typically define a posterior distribution over tree structures given data such as Dirichlet and Pitman-Yor diffusion trees [27, 22], coalescent models [36, 4, 20], and in the case of grouped data, the nested Chinese restaurant processes [2] and nested hierarchical Dirichlet processes [28]. Other models, such as tree structured nested sticking breaking, provide a distribution over a different class of tree structures, one for which data can sit at internal nodes [17]. These methods, while providing a distribution over trees, only support using parametric distributions to define emission probabilities and do not support the general family of probabilistic models used in our approach, which can use any scoring function to define the distribution. Factor graph-based distributions over tree structures such as [40] on the other hand support a flexible class of distributions over tree structures as in our approach. However inference in factor graph models as well as many of the Bayesian non-parameteric models is typically approximate or performed by sampling methods. This lends in practice to approximate MAP solutions and distributions over tree structures. Exact methods like the one proposed in this paper have not, to our knowledge, been proposed.

Dasgupta [16] defines a cost function for hierarchical clustering. Much work has been done to develop approximate solution methods and related objectives [30, 11, 7, 26, 10, 8].

Bootstrapping methods, such as [35], represent uncertainty in hierarchical clustering. Unlike our approach, bootstrapping methods approximate statistics of interest through repeatedly (re-)sampling from the empirical distribution.

Work on exact inference and exact distributions over flat clusterings [18], provides the foundation of our dynamic programming approach. Other work on exact flat clustering uses fast convolutions via the Möbius transform and Möbius inversion [23]. Kappes et al. [21] produce approximate distributions over flat clusterings using Perturb and MAP [29].

6 Conclusion

This paper describes a data structure and dynamic-programming algorithm to efficiently compute and sample from probability distributions over hierarchical clusterings. Our method improves upon the computation cost of brute-force methods from $(2N - 3)!!$ to sub-quadratic in the substantially smaller powerset of N . We demonstrate our methods' utility on jet physics and cancer genomics datasets, as well as a dataset related to Dasgupta's cost [16], and show its improvement over approximate methods. Finally, though there are multiple approaches to sample from the posterior distribution, such as MCMC techniques, they could be very expensive while our sampling method has a bounded computation time.

Acknowledgements

Kyle Cranmer and Sebastian Macaluso are supported by the National Science Foundation under the awards ACI-1450310 and OAC-1836650 and by the Moore-Sloan data science environment at NYU. Patrick Flaherty is supported in part by NSF HDR TRIPODS award 1934846. Andrew McCallum and Nicholas Monath are supported in part by the Center for Data Science and the Center for Intelligent Information Retrieval, and in part by the National Science Foundation under Grant No. NSF-1763618. Any opinions, findings and conclusions or recommendations expressed in this material are those of the authors and do not necessarily reflect those of the sponsor.

References

- [1] N. Bansal, A. Blum, and S. Chawla. Correlation clustering. *Machine learning*, 56(1-3): 89–113, 2004.
- [2] D. M. Blei, T. L. Griffiths, and M. I. Jordan. The nested chinese restaurant process and bayesian nonparametric inference of topic hierarchies. *Journal of the ACM (JACM)*, 2010.
- [3] C. Blundell, Y. Teh, and K. Heller. Bayesian rose trees. In *Uncertainty in Artificial Intelligence, (UAI)*, 2010.
- [4] L. Boyles and M. Welling. The time-marginalized coalescent prior for hierarchical clustering. In *Advances in Neural Information Processing Systems*, pages 2969–2977, 2012.
- [5] M. Cacciari, G. P. Salam, and G. Soyez. The anti- k_t jet clustering algorithm. *JHEP*, 04:063, 2008. doi: 10.1088/1126-6708/2008/04/063.
- [6] D. Callan. A combinatorial survey of identities for the double factorial, 2009.

- [7] M. Charikar and V. Chatziafratis. Approximate hierarchical clustering via sparsest cut and spreading metrics. In *Proceedings of the Twenty-Eighth Annual ACM-SIAM Symposium on Discrete Algorithms*, pages 841–854. SIAM, 2017.
- [8] M. Charikar, V. Chatziafratis, and R. Niazadeh. Hierarchical clustering better than average-linkage. In *Proceedings of the Thirtieth Annual ACM-SIAM Symposium on Discrete Algorithms*, pages 2291–2304. SIAM, 2019.
- [9] P. Cimiano and S. Staab. Learning concept hierarchies from text with a guided agglomerative clustering algorithm. In *Proceedings of the ICML 2005 Workshop on Learning and Extending Lexical Ontologies with Machine Learning Methods*, 2005.
- [10] V. Cohen-Addad, V. Kanade, and F. Mallmann-Trenn. Hierarchical clustering beyond the worst-case. In *Advances in Neural Information Processing Systems (NeurIPS)*, 2017.
- [11] V. Cohen-Addad, V. Kanade, F. Mallmann-Trenn, and C. Mathieu. Hierarchical clustering: Objective functions and algorithms. *Journal of the ACM (JACM)*, 66(4):1–42, 2019.
- [12] K. Cranmer, S. Macaluso, and D. Pappadopulo. Toy Generative Model for Jets, 2019. Toy Generative Model for Jets.
- [13] K. Cranmer, S. Macaluso, and D. Pappadopulo. Toy Generative Model for Jets Package, 2019. <https://github.com/SebastianMacaluso/ToyJetsShower>.
- [14] K. Cranmer, S. Macaluso, and D. Pappadopulo. Generation and Inference Unification in Jet Physics, 2020. Work in progress.
- [15] E. Dale and J. Moon. The permuted analogues of three Catalan sets, 1993.
- [16] S. Dasgupta. A cost function for similarity-based hierarchical clustering. In *Symposium on Theory of Computing (STOC)*, 2016.
- [17] Z. Ghahramani, M. I. Jordan, and R. P. Adams. Tree-structured stick breaking for hierarchical data. In *Advances in neural information processing systems*, pages 19–27, 2010.
- [18] C. Greenberg, N. Monath, A. Kobren, P. Flaherty, A. McGregor, and A. McCalum. Compact representation of uncertainty in clustering. In S. Bengio, H. Wallach, H. Larochelle, K. Grauman, N. Cesa-Bianchi, and R. Garnett, editors, *Advances in Neural Information Processing Systems 31*, pages 8630–8640. Curran Associates, Inc., 2018. <http://papers.nips.cc/paper/8081-compact-representation-of-uncertainty-in-clustering.pdf>.

- [19] C. Greenberg, N. Monath, A. Kobren, P. Flaherty, A. McGregor, and A. McCallum. Compact representation of uncertainty in clustering. In *Advances in Neural Information Processing Systems (NeurIPS)*. 2018.
- [20] Y. Hu, J. L. Ying, H. Daume III, and Z. I. Ying. Binary to bushy: Bayesian hierarchical clustering with the beta coalescent. In *Advances in Neural Information Processing Systems (NeurIPS)*, 2013.
- [21] J. H. Kappes, P. Swoboda, B. Savchynskyy, T. Hazan, and C. Schnörr. Probabilistic correlation clustering and image partitioning using perturbed multicut. In *International Conference on Scale Space and Variational Methods in Computer Vision*, 2015.
- [22] D. A. Knowles and Z. Ghahramani. Pitman-yor diffusion trees. In *Conference on Uncertainty in Artificial Intelligence (UAI)*, 2011.
- [23] J. Kohonen and J. Corander. Computing exact clustering posteriors with subset convolution. *Communications in Statistics-Theory and Methods*, 2016.
- [24] A. Kraskov, H. Stögbauer, R. G. Andrzejak, and P. Grassberger. Hierarchical clustering using mutual information. *EPL (Europhysics Letters)*, 70(2):278, 2005.
- [25] G. Louppe, K. Cho, C. Becot, and K. Cranmer. QCD-Aware Recursive Neural Networks for Jet Physics. *JHEP*, 01:057, 2019. doi: 10.1007/JHEP01(2019)057.
- [26] B. Moseley and J. Wang. Approximation bounds for hierarchical clustering: Average linkage, bisecting k-means, and local search. In *Advances in Neural Information Processing Systems*, 2017.
- [27] R. M. Neal. Density modeling and clustering using dirichlet diffusion trees. *Bayesian statistics*, 2003.
- [28] J. Paisley, C. Wang, D. M. Blei, and M. I. Jordan. Nested hierarchical dirichlet processes. *IEEE Transactions on Pattern Analysis and Machine Intelligence*, 2014.
- [29] G. Papandreou and A. L. Yuille. Perturb-and-map random fields: Using discrete optimization to learn and sample from energy models. In *2011 International Conference on Computer Vision*, pages 193–200. IEEE, 2011.
- [30] A. Roy and S. Pokutta. Hierarchical clustering via spreading metrics. *The Journal of Machine Learning Research*, 18(1):3077–3111, 2017.
- [31] D. E. Soper and M. Spannowsky. Finding physics signals with shower deconstruction. *Phys. Rev.*, D84:074002, 2011. doi: 10.1103/PhysRevD.84.074002.
- [32] D. E. Soper and M. Spannowsky. Finding top quarks with shower deconstruction. *Phys. Rev.*, D87:054012, 2013. doi: 10.1103/PhysRevD.87.054012.

- [33] T. Sørlie, C. M. Perou, R. Tibshirani, T. Aas, S. Geisler, H. Johnsen, T. Hastie, M. B. Eisen, M. Van De Rijn, S. S. Jeffrey, et al. Gene expression patterns of breast carcinomas distinguish tumor subclasses with clinical implications. *Proceedings of the National Academy of Sciences*, 98(19):10869–10874, 2001.
- [34] M. A. Suchard, P. Lemey, G. Baele, D. L. Ayres, A. J. Drummond, and A. Rambaut. Bayesian phylogenetic and phylodynamic data integration using beast 1.10. *Virus evolution*, 2018.
- [35] R. Suzuki and H. Shimodaira. Pvclust: an r package for assessing the uncertainty in hierarchical clustering. *Bioinformatics*, 22(12):1540–1542, 2006.
- [36] Y. W. Teh, H. Daume III, and D. M. Roy. Bayesian agglomerative clustering with coalescents. In *Advances in Neural Information Processing Systems (NeurIPS)*, 2008.
- [37] University of North Carolina. UNC microarray database, 2020. <https://genome.unc.edu/>.
- [38] B. Van Os and J. J. Meulman. Improving dynamic programming strategies for partitioning. *Journal of classification*, 21(2):207–230, 2004.
- [39] L. Wang, A. Bouchard-Côté, and A. Doucet. Bayesian phylogenetic inference using a combinatorial sequential monte carlo method. *Journal of the American Statistical Association*, 110(512):1362–1374, 2015.
- [40] M. Wick, S. Singh, and A. McCallum. A discriminative hierarchical model for fast coreference at large scale. In *Association for Computational Linguistics (ACL)*, 2012.

A Appendix

A.1 Proof of Proposition 1

Proof. Given a dataset X , pick an element $x \in X$. We consider all possible Ω clusters $X_L^\omega \subset X$ that contain x . Given X_L^ω , then X_R^ω is fixed so as to satisfy $X_L^\omega \cup X_R^\omega = X$ and $X_L^\omega \cap X_R^\omega = \emptyset$. We want to show that the partition function $Z(X)$ can be written recursively in terms of $Z(X_L^\omega)$ and $Z(X_R^\omega)$.

The partition function is defined as the sum of the energies of all possible hierarchical clusterings $\mathcal{H}_X = \{\mathbb{H}^m\}_{m=1}^M$,

$$\begin{aligned} Z(X) &= \sum_{m=1}^M \phi(\mathbb{H}^m(X)) \\ &= \sum_{m=1}^M \psi(X_L^m, X_R^m) \phi(\mathbb{H}^m(X_L^m)) \phi(\mathbb{H}^m(X_R^m)) \end{aligned} \quad (9)$$

where $X_L^m \cup X_R^m = X$, $X_L^m \cap X_R^m = \emptyset$. Also, $\mathbb{H}^m(X_L^m)$ and $\mathbb{H}^m(X_R^m)$ are the sub-hierarchies in \mathbb{H}^m that are rooted at X_L^m and X_R^m , respectively. Next, we rewrite Eq. 9 grouping together all the hierarchies \mathbb{H}^i that have the same clusters $\{X_L^m, X_R^m\}$ ²,

$$\begin{aligned} Z(X) &= \sum_{\omega=1}^{\Omega} \psi(X_L^\omega, X_R^\omega) \sum_{j=1}^J \phi(\mathbb{H}^j(X_L^\omega)) \sum_{k=1}^K \phi(\mathbb{H}^k(X_R^\omega)) \\ &= \sum_{\omega=1}^{\Omega} \psi(X_L^\omega, X_R^\omega) Z(X_L^\omega) Z(X_R^\omega) \end{aligned} \quad (10)$$

with $M = \Omega \cdot J \cdot K$, $J = (2|X_L^\omega| - 3)!!$, and $K = (2|X_R^\omega| - 3)!!$. Thus, $Z(X)$ of a cluster X can be written recursively in terms of the partition function of the sub-clusters of X ³. □

A.2 Proof of Theorem 2

Proof. We want to show that drawing samples of trees using Algorithm 2 gives samples from $P(\mathbb{H}|X)$. To do this, we show that the probability of a tree can be re-written as the product of probabilities of sampling each split in the structure. This then directly corresponds to the top-down sampling procedure in Algorithm 2.

²The cluster trellis provides an exact solution conditioned on the fact that the domain of the linkage function is the set of pairs of clusters, and not pairs of trees.

³Note that for each singleton x_i , we have $Z(x_i) = 1$.

Recall from Definition 2 we have:

$$P(\mathbb{H}|X) = \frac{1}{Z(X)} \prod_{X_L, X_R \in \text{sibs}(\mathbb{H})} \psi(X_L, X_R) \quad (11)$$

We can equivalently write this as:

$$P(\mathbb{H}|X) = \prod_{X_L, X_R \in \text{sibs}(\mathbb{H})} \frac{1}{Z(X_L \cup X_R)} \cdot \psi(X_L, X_R) \cdot Z(X_L) \cdot Z(X_R) \quad (12)$$

To understand why this can be written this way, observe that for each in $\text{sibs}(H)$ (i.e., internal nodes such as X_L and X_R the $Z(X_L)$ and $Z(X_R)$ terms will be cancelled out by corresponding terms in the product for the children of X_L or X_R . To see this we can write out the product for three pairs nodes X_L, X_R and their children X_{LL}, X_{LR} and X_{RL} and X_{RR} respectively:

$$\frac{1}{Z(X_p)} \psi(X_L, X_R) Z(X_L) Z(X_R) \cdot \frac{1}{Z(X_L)} \psi(X_{LL}, X_{LR}) Z(X_{LL}) Z(X_{LR}) \cdot \frac{1}{Z(X_R)} \psi(X_{RL}, X_{RR}) Z(X_{RL}) Z(X_{RR}) \quad (13)$$

Recall that for the pair of siblings that are the children of the root that the $\frac{1}{Z(X_L \cup X_R)}$ term will not be cancelled out and corresponds exactly to $\frac{1}{Z(X)}$ the partition function.

Next, we observe that Eq. 12 can be re-written in terms of Equation 8 which defines $p(X_L|X_L \cup X_R)$:

$$P(\mathbb{H}|X) = \prod_{X_L, X_R \in \text{sibs}(\mathbb{H})} p(X_L|X_L \cup X_R) \quad (14)$$

Algorithm 2 applies Eq. 8 recursively in a top-down manner using a series of splits which have a probability that directly corresponds to the product of terms in Eq. 14. \square

A.3 Proof of Lower Bound on Number of Trees

The number of trees on N leaves is given exactly by $\frac{\prod_{i=1}^{N-1} m_i}{(N-1)!} \prod_{i=2}^N \binom{i}{2}$, where m_i is the number of internal nodes in the subtree rooted at node i [4]. Since $\prod_{i=2}^N \binom{i}{2} = \frac{N!^2}{N*2^{N-1}}$, this makes the number of trees on N leaves $\frac{\prod_{i=1}^{N-1} m_i}{(N-1)!} \frac{N!^2}{N*2^{N-1}} = \frac{\prod_{i=1}^{N-1} m_i * N * N!}{N*2^{N-1}} = \frac{\prod_{i=1}^{N-1} m_i * N!}{2^{N-1}}$. The smallest conceivable value for $\prod_{i=1}^{N-1} m_i = \omega(N)$, which gives us the bound on the number of trees to be $\omega(NN!/2^{N-1})$, as desired.

Note that this is a loose lower-bound, and that it could be improved upon as follows: say a hierarchical clustering is a *caterpillar clustering* if every internal node in the underlying

tree has two children and the set associated with one of those children as size one. There are $n!/2$ caterpillar clustering. To see this, note that the i th level (where the root is level 1) of a caterpillar clustering has exactly one leaf for $i = 2, \dots, n-1$. There are $n(n-1)\dots 3 = n!/2$ choices for the corresponding singleton sets.

Note, however, that there is a closed form expression for the exact number of unordered hierarchies given by $a(N) = (2N-3)!!$, with n the number of singletons (see [6, 15] for more details and proof).

A.4 Correctness Proof of Marginal Algorithms

A.4.1 Sub-Hierarchy Marginal

For a given sub-hierarchy rooted at X_i , i.e., $\mathbb{H}_i \in \mathcal{H}(X_i)$, the marginal probability is defined as $P(\mathbb{H}_i|X) = \sum_{\mathbb{H} \in A(\mathbb{H}_i)} P(\mathbb{H}|X)$, where $A(\mathbb{H}_i) = \{\mathbb{H} : \mathbb{H} \in \mathcal{H}(X) \wedge \mathbb{H}_i \subset \mathbb{H}\}$, and $\mathbb{H}_i \subset \mathbb{H}$ indicates that \mathbb{H}_i is a subtree of \mathbb{H} . We can rewrite $\sum_{\mathbb{H} \in A(\mathbb{H}_i)} P(\mathbb{H}|X)$ as $\sum_{\mathbb{H} \in A(\mathbb{H}_i)} \phi(\mathbb{H}(X))/Z$, which gives us:

$$P(\mathbb{H}_i|X) = \sum_{\mathbb{H} \in A(\mathbb{H}_i)} P(\mathbb{H}|X) = \sum_{\mathbb{H} \in A(\mathbb{H}_i)} \frac{\phi(\mathbb{H}(X))}{Z} = \frac{Z_{\mathbb{H}_i}(X)}{Z} \quad (15)$$

where $Z_{\mathbb{H}_i}(X) = \sum_{\mathbb{H} \in A(\mathbb{H}_i)} \phi(\mathbb{H}(X))$, the sum of potential values for all the hierarchies containing the sub-hierarchy \mathbb{H}_i . This gives us

$$\begin{aligned} Z_{\mathbb{H}_i}(X) &= \sum_{m=1}^{|A(\mathbb{H}_i)|} \phi(\mathbb{H}^m(X)) \\ &= \sum_{m=1}^{|A(\mathbb{H}_i)|} \psi(X_L^m, X_R^m) \phi(\mathbb{H}^m(X_L^m)) \phi(\mathbb{H}^m(X_R^m)) \end{aligned} \quad (16)$$

where $X_L^m \cup X_R^m = X$, $X_L^m \cap X_R^m = \emptyset$. Also, $\mathbb{H}^m(X_L^m)$ and $\mathbb{H}^m(X_R^m)$ are the sub-hierarchies in \mathbb{H}^m that are rooted at X_L^m and X_R^m , respectively. Next, we rewrite Eq. 16 grouping together all the hierarchies \mathbb{H}^i that have the same clusters $\{X_L^m, X_R^m\}$. Note that $\mathbb{H}_i \subset \mathbb{H}$, implies $X_i \subseteq X_L$ or $X_i \subseteq X_R$. Assume W.L.O.G. that $X_i \subseteq X_L$.

$$\begin{aligned} Z_{\mathbb{H}_i}(X) &= \sum_{\omega=1}^{\Omega} \psi(X_L^\omega, X_R^\omega) \sum_{j=1}^J \phi(\mathbb{H}^j(X_L^\omega)) \sum_{k=1}^K \phi(\mathbb{H}^k(X_R^\omega)) \\ &= \sum_{\omega=1}^{\Omega} \psi(X_L^\omega, X_R^\omega) Z_{\mathbb{H}_i}(X_L^\omega) Z(X_R^\omega) \end{aligned} \quad (17)$$

with $|A(\mathbb{H}_i)| = \Omega \cdot J \cdot K$, $J = |\{\mathcal{H}(X_L) : X_i \subseteq X_L\}|$, $K = |\{\mathcal{H}(X_R)\}|$ and setting $Z_{\mathbb{H}_i}(X_i) = \phi(\mathbb{H}(X_i))$.

A.4.2 Subset Marginal

For a given cluster X_i , the marginal probability is defined as $P(X_i|X) = \sum_{\mathbb{H} \in A(X_i)} P(\mathbb{H}|X)$, where $A(X_i) = \{\mathbb{H} : \mathbb{H} \in \mathcal{H}(X) \wedge X_i \subset \mathbb{H}\}$, and $X_i \subset \mathbb{H}$ indicates that cluster X_i is contained in \mathbb{H} . We can rewrite $\sum_{\mathbb{H} \in A(X_i)} P(\mathbb{H}|X)$ as $\sum_{\mathbb{H} \in A(X_i)} \phi(\mathbb{H}(X))/Z$, which gives us:

$$P(X_i|X) = \sum_{\mathbb{H} \in A(X_i)} P(\mathbb{H}|X) = \sum_{\mathbb{H} \in A(X_i)} \frac{\phi(\mathbb{H}(X))}{Z} = \frac{Z_{X_i}(X)}{Z} \quad (18)$$

where $Z_{X_i}(X) = \sum_{\mathbb{H} \in A(X_i)} \phi(\mathbb{H}(X))$, the sum of potential values for all the hierarchies containing the cluster X_i . This gives us

$$\begin{aligned} Z_{X_i}(X) &= \sum_{m=1}^{|A(X_i)|} \phi(\mathbb{H}^m(X)) \\ &= \sum_{m=1}^{|A(X_i)|} \psi(X_L^m, X_R^m) \phi(\mathbb{H}^m(X_L^m)) \phi(\mathbb{H}^m(X_R^m)) \end{aligned} \quad (19)$$

where $X_L^m \cup X_R^m = X$, $X_L^m \cap X_R^m = \emptyset$. Also, $\mathbb{H}^m(X_L^m)$ and $\mathbb{H}^m(X_R^m)$ are the sub-hierarchies in \mathbb{H}^m that are rooted at X_L^m and X_R^m , respectively. Next, we rewrite Eq. 19 grouping together all the hierarchies \mathbb{H}^i that have the same clusters $\{X_L^m, X_R^m\}$. Note that $X_i \subset \mathbb{H}$, implies $X_i \subseteq X_L$ or $X_i \subseteq X_R$. Assume W.L.O.G. that $X_i \subseteq X_L$.

$$\begin{aligned} Z_{X_i}(X) &= \sum_{\omega=1}^{\Omega} \psi(X_L^\omega, X_R^\omega) \sum_{j=1}^J \phi(\mathbb{H}^j(X_L^\omega)) \sum_{k=1}^K \phi(\mathbb{H}^k(X_R^\omega)) \\ &= \sum_{\omega=1}^{\Omega} \psi(X_L^\omega, X_R^\omega) Z_{X_i}(X_L^\omega) Z(X_R^\omega) \end{aligned} \quad (20)$$

with $|A(\mathbb{H}_i)| = \Omega \cdot J \cdot K$, $J = |\{\mathcal{H}(X_L) : X_i \subseteq X_L\}|$, $K = |\{\mathcal{H}(X_R)\}|$, and setting $Z_{X_i}(X_i) = Z(X_i)$.

A.5 Proof of MAP Time Complexity

The MAP tree is computed for each node in the trellis, and due to the order of computation, at the time of computation for node i , the MAP trees for all nodes in the subtrellis rooted at node i have already been computed. Therefore, the MAP tree for a node with i elements can be computed in 2^i steps (given the pre-computed partition functions for each of the node's descendants), since the number of nodes for the trellis rooted at node i (with i elements) corresponds to the powerset of i . There are $\binom{n}{i}$ nodes of size i , making the total computation $\sum_{i=1}^N 2^i \binom{n}{i} = 3^N - 1$.

Algorithm 3 $\text{MAP}(X)$

```

if  $\phi(\mathbb{V}(X))$  set then
    return  $\phi(X), \Xi(X)$ 
Pick  $x_i \in X$ 
 $\phi(X) \leftarrow -\infty$ 
 $\Xi(X) \leftarrow \text{null}$  {Backpointer to give MAP tree structure.}
for  $X_j$  in  $2^{X \setminus \{x_i\}}$  do
     $X_i \leftarrow X_j \cup \{x_i\}$ 
     $t \leftarrow \psi(X_i, X \setminus X_i) \cdot \phi(\mathbb{V}(X_i)) \cdot \phi(\mathbb{V}(X \setminus X_i))$ 
    if  $\phi(X) < t$  then
         $\phi(X) \leftarrow t$ 
         $\Xi(X) \leftarrow \{X_i, X \setminus X_i\} \cup \Xi(X_i) \cup \Xi(X \setminus X_i)$ 
return  $\phi(X), \Xi(X)$ 

```

A.6 Proof of Proposition 2

Proof. We proceed in a similar way as detailed in Appendix § A.1, as follows. Given a dataset X , pick an element $x \in X$. We consider all possible Ω clusters $X_L^\omega \subset X$ that contain x . Given X_L^ω , then X_R^ω is fixed so as to satisfy $X_L^\omega \cup X_R^\omega = X$ and $X_L^\omega \cap X_R^\omega = \emptyset$. We want to show that the MAP clustering $\phi(\mathbb{H}^*(X))$ can be computed recursively in terms of $\phi(\mathbb{H}^*(X_L^\omega))$ and $\phi(\mathbb{H}^*(X_R^\omega))$.

The MAP value is defined as the energy of the clustering with maximal energy ϕ among all possible hierarchical clusterings $\mathcal{H}_X = \{\mathbb{H}^m\}_{m=1}^M$,

$$\begin{aligned}
\phi(\mathbb{H}^*(X)) &= \max_{m \in M} \phi(\mathbb{H}^m(X)) \\
&= \max_{m \in M} \psi(X_L^m, X_R^m) \phi(\mathbb{H}^m(X_L^m)) \phi(\mathbb{H}^m(X_R^m))
\end{aligned} \tag{21}$$

where $X_L^m \cup X_R^m = X$, $X_L^m \cap X_R^m = \emptyset$. Also, $\mathbb{H}^m(X_L^m)$ and $\mathbb{H}^m(X_R^m)$ are the sub-hierarchies in \mathbb{H}^m that are rooted at X_L^m and X_R^m , respectively. As mentioned earlier, the cluster trellis provides an exact MAP solution conditioned on the fact that the domain of the linkage function is the set of pairs of clusters, and not pairs of trees. Thus, we can rewrite Eq. 21 grouping together all the hierarchies \mathbb{H}^i that have the same clusters $\{X_L^m, X_R^m\}$, as follows

$$\begin{aligned}
\phi(\mathbb{H}^*(X)) &= \max_{\omega \in \Omega} \left(\psi(X_L^\omega, X_R^\omega) * \right. \\
&\quad \left. \max_{j \in J} \phi(\mathbb{H}^j(X_L^\omega)) \max_{k \in K} \phi(\mathbb{H}^k(X_R^\omega)) \right) \\
&= \max_{\omega \in \Omega} \psi(X_L^\omega, X_R^\omega) \phi(\mathbb{H}^*(X_L^\omega)) \phi(\mathbb{H}^*(X_R^\omega))
\end{aligned} \tag{22}$$

with $M = \Omega \cdot J \cdot K$. Thus, $\phi(\mathbb{H}^*(X))$ of a cluster X can be written recursively in terms of the MAP values of the sub-clusters of X ⁴.

□

A.7 Proof of Theorem 1

The partition function is computed for each node in the trellis, and due to the order of computation, at the time of computation for node i , the partition functions for all nodes in the subtrellis rooted at node i have already been computed. Therefore, the partition function for a node with i elements can be computed in 2^i steps (given the pre-computed partition functions for each of the node's descendants), since the number of nodes for the trellis rooted at node i (with i elements) corresponds to the powerset of i . There are $\binom{n}{i}$ nodes of size i , making the total computation $\sum_{i=1}^N 2^i \binom{n}{i} = 3^N - 1$.

A.8 Additional Details on PAM50 Experiments

The Pearson correlation coefficient was used for the clustering metric for the PAM50 data set experiments. The correlation clustering input can be represented as a complete weighted graph, $G = (V, E)$, where each edge has weight $w_{uv} \in [-1, 1], \forall (u, v) \in E$. The goal is to construct a clustering of the nodes that maximizes the sum of positive within-cluster edge weights minus the sum of all negative across-cluster edge weights. However, the correlations among subsampled pam50 ($n = 12$) data set are all positive. To allow more balanced weights among vertices, we transform the weights using $w'_{uv} = \tan(w_{uv} \frac{\pi}{2})$ and then subtracted the average of all w'_{uv} .

A.9 Jet Physics Background

It is natural to represent a jet and the particular clustering history that gave rise to it as a binary tree, where the inner nodes represent each of the unstable particles and the leaves represent the jet constituents. This representation connects jets physics with natural language processing (NLP) and biology, which is exciting and was first suggested in [25].

Jets are among the most common objects produced at the Large Hadron Collider (LHC) at CERN, and a great amount of work has been done to develop techniques for a better treatment and understanding of them, from both an experimental and theoretical point of view. In particular, determining the nature (type) of the initial unstable particle (the root of the binary tree), and its children and grandchildren that gave rise to a specific jet is essential in searches for new physics, as well as precision measurements of our current model of nature, i.e., the Standard Model of particle physics. In this context, it becomes relevant and interesting to study algorithms to cluster the jet constituents (leaves) into a binary tree and metrics to compare them. Being able to improve over the current techniques that

⁴Note that for each singleton x_i , we have $\phi(\mathbb{H}^*(x_i)) = 1$.

attempt to invert the showering process to reconstruct the ground truth-level tree would assist in physics searches at the Large Hadron Collider.

There are software tools called **parton showers**, e.g., PYTHIA, Herwig, Sherpa, that encode a physics model for the simulation of jets that are produced at the LHC. Current algorithms used by the physics community to estimate the clustering history of a jet are domain-specific sequential recombination jet algorithms, called *generalized k_t clustering algorithms* [5], and they do not use these generative models. These algorithms sequentially cluster the jet constituents by locally choosing the pairing of nodes that minimizes a distance measure. Given a pair of nodes, this measure depends on the angular distance between their momentum vector and the value of this vector in the transverse direction with respect to the collision axis between the incoming beams of protons.

Currently, generative models that implement the parton shower in full physics simulations are implicit models, i.e., they do not admit a tractable density. Extracting additional information that describes the features of the latent process is relevant to study problems where we aim to unify generation and inference, e.g inverting the generative model to estimate the clustering history of a jet. A schematic representation of this approach is shown in Figure 6.

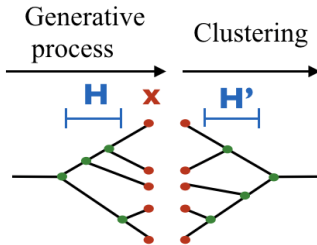


Figure 6: Schematic representation of the tree structure of a sample jet generated with Ginkgo and the clustered tree for some clustering algorithm. For a given algorithm, z labels the different variables that determine the latent structure of the tree. The tree leaves x are labeled in red and the inner nodes in green.

At present, it is very hard to access the joint likelihood in state-of-the-art parton shower generators in full physics simulations. Also, typical implementations of parton showers involve sampling procedures that destroy the analytic control of the joint likelihood. Thus, to aid in machine learning (ML) research for jet physics, a python package for a toy generative model of a parton shower, called Ginkgo, was introduced in [13]. Ginkgo has a tractable joint likelihood, and is as simple and easy to describe as possible but at the same time captures the essential ingredients of parton shower generators in full physics simulations. Within the analogy between jets and NLP, Ginkgo can be thought of as ground-truth parse trees with a known language model. A python package with a pyro implementation of the model with few software dependencies is publicly available in [13].

A.10 Counting Trees

We count the total number of hierarchies⁵. We implement a bottom-up approach and start by assigning a number of trees $N = 1$ to each cluster of one element. Then, given a parent cluster X_p , we add the contribution N_p^i ($N_p = \sum_i N_p^i$) of each possible pair i of left and right children, $s_{X_p} = \{X_L, X_R\}$, where $X_L \cup X_R = X_p$ and $X_L \cap X_R = \emptyset$. In particular, we obtain

$$N_p^i = N_{X_L}^i \cdot N_{X_R}^i \quad (23)$$

Thus N_p is the number of possible trees of the sub-branch whose root node is X_p . We repeat the process until we reach the cluster of all elements X .

A.11 Runtime Asymptotics Plots

See Figure 7 for a comparison of the number of trees vs the time complexity of the trellis algorithms for finding the partition function, MAP, and marginal values.

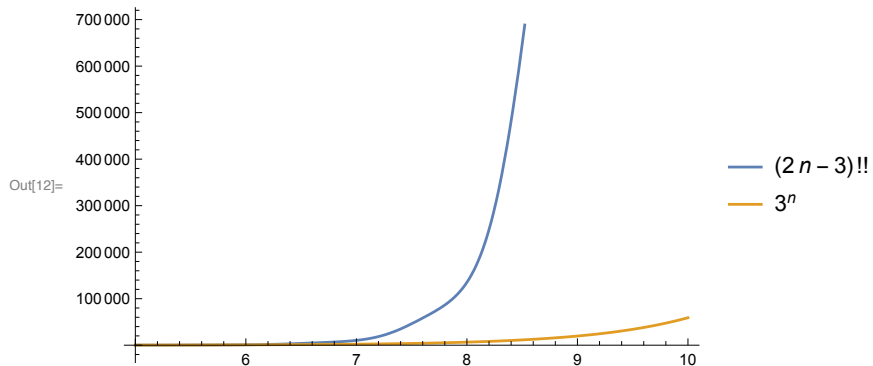
A.12 Description of Computer Architecture and Experimental Runtime

When using a MacBook Pro with a 2.5 GHz Intel Core i5 processor with 8GB 1600 MHz DDR3 RAM to compute the MAP for the genetics experiments using the PAM dataset, it takes approximately 15 minutes to complete from start to finish (including data loading and result output). When using this same machine to compute that MAP for Dasgupta cost on the given graph, it takes approximately 4 seconds to complete from start to finish (including data loading and result output).

When using a MacBook Pro with a 2.3 GHz Intel Core i9 processor with 16GB 2400 MHz DDR4 RAM to compute the MAP for the jet physics experiments it takes 5×10^{-2} , 1.6 and 6.1 seconds to run the trellis on jets with 5, 9 and 10 leaves respectively.

⁵This gives a result matching exactly the formula $(2N - 3)!!$

```
In[12]:= Plot[{(2 n - 3) !!, 3^n}, {n, 5, 10}, PlotLegends → "Expressions"]
```



```
In[15]:= Plot[{(2 n - 3) !!, 3^n}, {n, 10, 15}, PlotLegends → "Expressions"]
```

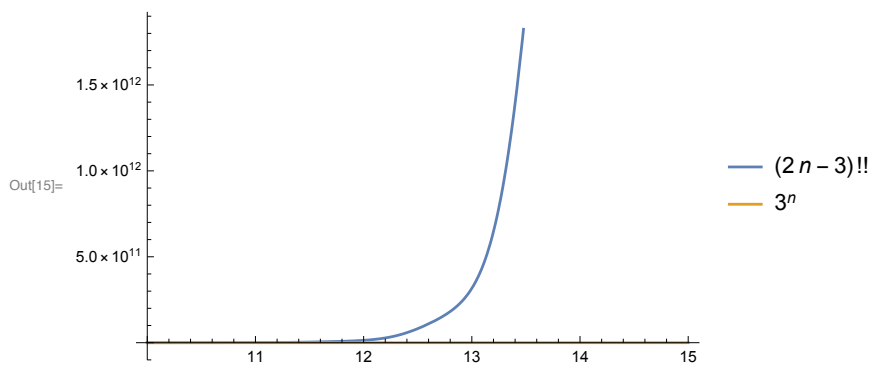


Figure 7: Comparison of the the number of trees vs complexity of trellis algorithms.